Ionics (2012) 18:291–297
DOI 10.1007/s11581-011-0633-4

ORIGINAL PAPER

The effect of strontium doping on densification and electrical properties of $Ce_{0.8}Gd_{0.2}O_{2-\delta}$ electrolyte for IT-SOFC application

Buchi Suresh M. · Johnson Roy

Received: 21 June 2011 / Revised: 31 August 2011 / Accepted: 22 September 2011 / Published online: 6 October 2011

Abstract The effect of strontium doping on densification and ionic conductivity of gadolinium-doped ceria (GDC) was investigated. Doped (Sr-GDC) and un-doped GDC green specimens were subjected to dilatometric measurements to evaluate their sintering behavior and to identify the sintering temperature regimes. XRD spectra show the crystal structure of the sintered samples to be cubic. Strontium doping has exhibited a relatively larger grain size as is evident by the microstructural characterization. AC impedance analysis exhibited a threefold increase in ionic conductivity for Sr-GDC (0.072 S/cm) in comparison to GDC (0.028 S/cm) samples which can be attributed to improved density and increased grain size, resulting in enhancement of total conductivity. Additionally, strontium doping to GDC lattice not only increases the oxygen vacancies but also decreases the lattice binding energy, leading to increase in oxygen ion mobility which is also confirmed by the lower activation energy exhibited by the Sr-GDC formulation. Our experimental results established that co-doping is very effective in identifying new materials with remarkably high ionic conductivity with substantial reduction in the cost for solid oxide fuel cell application.

Keywords Ceria · SOFCs · AC conductivities · Doping · Fuel cells

B. S. M. (✉) · J. Roy
Center for Ceramic Processing, International Advanced Research Centre for Powder Metallurgy and New Materials (ARCI), Hyderabad, AP, India 500005
e-mail: suresh@arci.res.in

J. Roy
e-mail: royjohnson@arci.res.in

Introduction

Solid oxide electrolytes with high conductivity of oxygen ion are of significant interest because of their potential application in fuel cells, electrochemical sensors, oxygen pumps, etc. Though yttria-stabilized zirconia is successfully used in solid oxide fuel cells (SOFCs), relatively low oxygen flux at low and intermediate temperature has become one of the major disadvantages which has opened up research on novel electrolyte materials. Out of the various electrolytes, ceria-based solid solutions $Ce_{1-x}M_xO_2$ (Me, Sm, and Gd) and x=0.15–0.20 have been regarded as promising electrolyte materials [1, 2]. However, CeO_2 poses processing difficulty of high sintering temperatures, above 1,500°C, to achieve close to theoretical density which is critical for successful performance. Another main drawback of ceria-based electrolytes, limiting their commercial application, is increased electronic conduction under low oxygen partial pressure accompanied by reduction of Ce^{4+} to Ce^{3+} [3]. It has been reported that reduction of ceria can be neglected at lower temperatures around 600–700°C. In order to address these problems, doping of ceria with suitable dopants, which impart structural and/or valency modifications, reduction in the lattice binding energy to improve oxygen ions migration is being attempted [4].

A significant change in electrical property was observed in $Ce_{0.8}(CaGdSm)_{0.2}O_2$ [5], $Ce_{0.8}Gd_{0.2-x}Pr_xO_{1.9}$ [6], $Ce_{0.8}Gd_{0.2-x}Sm_xO_{1.9}$ [7], $Ce_{1.9}Gd_{0.1}O_{1.95}$ adding 2 wt.% Co [8], $Ce_{0.85}Gd_{0.1}Mg_{0.05}O_{1.9}$ [9], $Ce_{1-a}Gd_{a-y}Sm_yO_{2-0.5a}$ [10], $Ce_{1-x-y}Sm_xLa_yO_{2-z}$ [11], and $Ce_{1-x-y}Y_xLa_yO_{2-z}$ [12] electrolytes. Zhang et al. have reported that Fe could also aid sintering for both pure and doped CeO_2 [13, 14]. Zhang

et al. reported that the grain conductivity of GDC20 (20 mol% Gd-doped CeO_2) increased by ~60% with alumina addition and the grain boundary conductivity rapidly decreased with alumina addition. They attributed the increase of grain conductivity to Gd content, assuming the solubility of Al is very low. That is, grain conductivity is dependent only on the composition of Gd and the decrease of the grain boundary conductivity may be attributed to $GdAlO_3$ [15]. It has been reported that the addition of a small amount of Mn appreciably reduces the sintering temperature. A similar effect has also been reported on systems of GDC20 doped with transition metal ions Co, Fe, and Cu [16, 17]. Lieinlogel and Gauckler have used cobalt as the sintering aid for gadolinium-doped CeO_2 (GDC) and found that GDC ($Ce_{0.8}Gd_{0.2}O_{1.9-\delta}$) with density higher than 99% could be obtained even when sintering at 900°C with 1 mol% Co_3O_4 addition [18].

In spite of many different strategies adopted for improving the properties of such oxides either by co-doping techniques or by using improved processing techniques, the desired advancements have not been achieved so far. Thus, considering the technological applications of materials displaying high oxide ion conductivity, we felt the need to explore novel cost-effective compositions that exhibit enhanced properties in the ceria family of oxides. Ionic radii compatibility of the dopant and the host cation is very critical in achieving the desired lattice match and, thereby, the properties. Moreover, the lattice binding energy of the dopant should be low. Thus, taking into consideration the critical factors that could, in principle, enhance the ionic conductivity, attempts were made to prepare a newer composition. In the present study, co-doping of strontium and gadolinium on CeO_2 electrolytes has been explored so that the average radii of the dopants will become close to the critical radii and average binding energy will be lowered as proposed for multiple doping [1]. Further, this study is relevant in view of the limited studies reported on the conduction behavior of strontium substituted in GDC system.

Experimental

Figure 1 shows the particle size analysis of commercially available high-purity (min. 99.9%) ultrafine GDC powder (Cottor International, India) of composition $Ce_{0.8}Gd_{0.2}O_{2-\delta}$ (GDC). The average particle size of the powder is 220 nm as is evident from dynamic light scattering measurements. GDC powder and GDC powder added with $SrCO_3$ (Fisher Scientific, India; min. 99.9%) in appropriate stoichiometry (1.2 mol%) were separately wet-milled in organic medium for 24 h using a ball milling machine (Mak Deal, India). The mixed powders were then dried and compacted after granulation into discs of 10 mm in diameter by applying 25 MPa of pressure using a hydraulic press (Peeco Hydraulic Pvt. Ltd, India) for preparation of the pellets. Polyvinylpyrolidene of 2 wt% was used as binder. The green compacts of GDC and Sr-GDC were subjected to dilatometric measurements (NETZSCH TMA, Germany) at a heating rate of 2°C/min up to 1,400°C to evaluate their sintering behavior and to identify the sintering temperature regimes. The compacts were further sintered at 1,400°C in a sintering air furnace for 2 h based on the dilatometric studies. The bulk density of the sintered

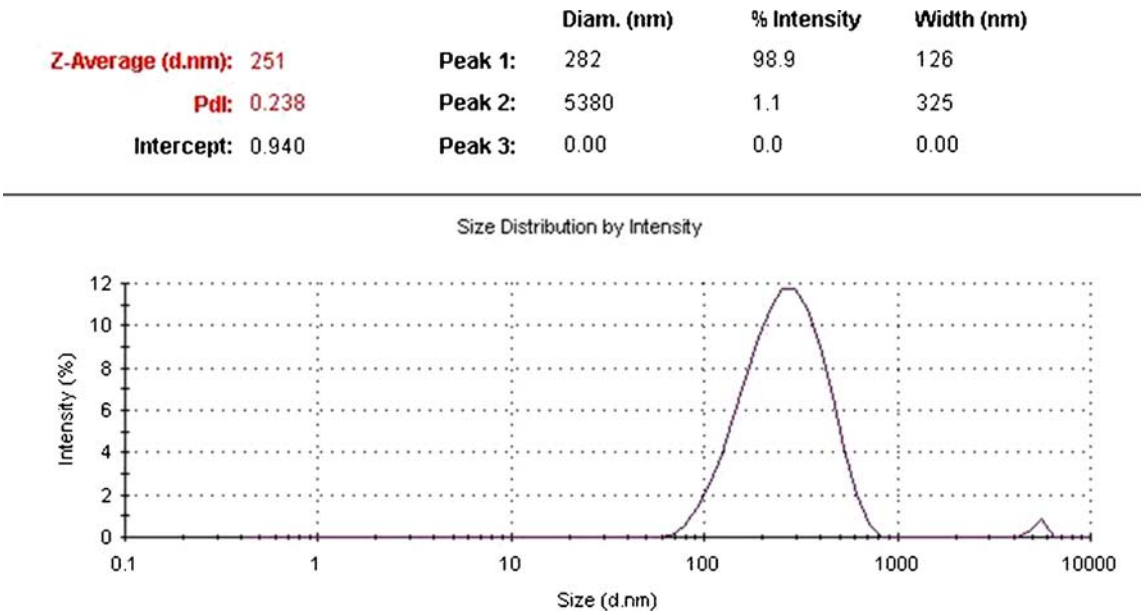

Fig. 1 Particle size analysis of GDC powder

specimens was determined by the Archimedes principle using a density determination balance. GDC ($Ce_{0.8}Gd_{0.2}O_{1.9-\delta}$) and Sr-GDC ($Ce_{0.79}Gd_{0.2}Sr_{0.01}O_{1.9-\delta}$) pellets were subjected to phase analysis using Bruker D8 Axs Advance X-ray diffractometer with Cu K_α radiation (λ=1.5406 Å) to confirm the phase formation.

The sintered pellets were mounted and polished using standard metallographic polishing and etching followed by their micro-structural evaluation using SEM (Hitachi S-3400N, Tokyo, Japan). The electrical conductivity of the sintered discs in air was measured by a four-probe two-point AC impedance method using AC impedance gain/phase analyzer (Solartron SI1260, Ametek, Inc., Hampshire, UK). To ensure a good contact between the platinum wires and the disc, each side of the disc was painted with platinum paste after they had been polished and annealed. Impedance measurements were made from 0.1 Hz to 10 MHz over temperature ranging 300–800°C at an excitation voltage of 100 mV for all temperatures and all frequencies.

Results and discussion

The X-ray diffraction patterns of the sintered GDC and Sr-GDC samples are presented in Fig. 2. XRD patterns have shown CeO_2 solid solution as the prominent cubic phase. However, the lattice parameter increases from 5.420 Å to 5.439 Å with the addition of Sr. This can be attributed to the volume expansion of the lattice due to the larger ionic radii of 1.26 Å for Sr^{2+} in comparison to Ce^{4+} with 0.96 Å. Doping of Sr^{2+} in ceria lattice will induce a uniform strain in the lattice as the material is elastically deformed. There is no indication of secondary phase formation as a result of Sr^{2+} addition, suggesting dissolution in the ceria lattice.

Dilatometric curves recorded for GDC and Sr-GDC samples are shown in Fig. 3. The curves indicated a significant increase in sintering rate from 700°C and reaching towards a minimum shrinkage rate as evidenced by no significant/negligible slope change. It is evident that the total shrinkage achieved is found to be higher in the case of Sr-GDC and is further confirmed by the final densities measured with Sr-GDC (98%) against 94% observed with GDC formulation. The higher densification observed with Sr^{2+} doping indicates that strontium acts as a sintering aid for achieving final density values close to theoretical ones. Thus, multiple doping is found to enhance the densification behavior of the sintered ceria ceramics compared to pure ceria [19].

The microstructure of the metallographically polished samples and fracture surface of the sintered pellets of GDC and Sr-GDC was studied by SEM as shown in Figs. 4a, b and 5a, b. Fractured surfaces in the case of sintered GDC pellets have shown more pores consistent with the measured density of the sintered pellets. It can be clearly observed in the micrographs that the samples have no cracks and deformations.

Impedance patterns recorded for GDC and Sr-GDC measured at 300, 350, 400, and 800°C in air are shown in Fig. 6a, d. The interpretation of impedance data for polycrystalline materials has been well documented. In general, the AC impedance of an ionic conductor measured by the two-probe method contains the contributions from grain interior, grain boundary, and electrode–electrolyte interface polarization, which are reflected in a complex plane with three successive arcs. In a practical case, however, not all of these arcs can be observed, depending on the nature of samples and the testing conditions. The addition of strontium to the GDC ceramic has almost no

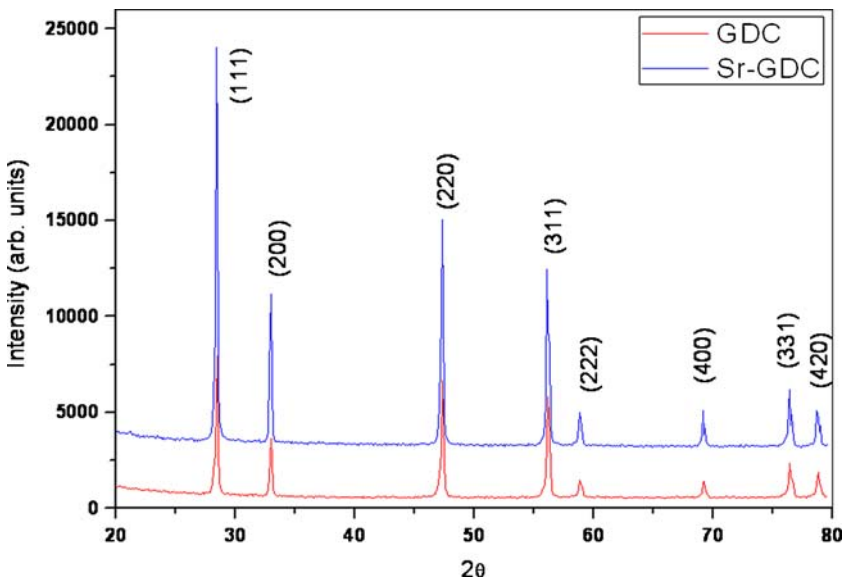

Fig. 2 X-ray diffraction pattern of GDC and Sr-GDC samples

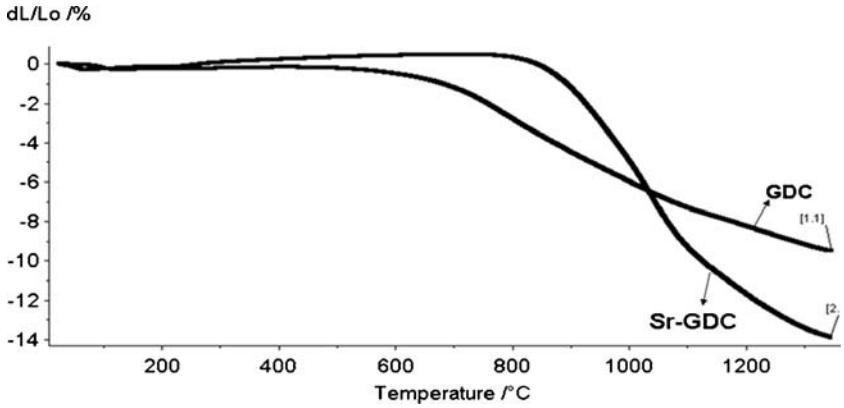

Fig. 3 Dilatometric curves recorded for GDC and Sr-GDC samples

effect on grain conduction but leads to a significant increase in grain boundary conductivity as shown in Fig. 6b. At 350°C, the grain boundary conductivity was substantially increased by one order with Sr addition from 6.85×10^{-6} S/cm for GDC to 3.4×10^{-5} S/cm for Sr-GDC. This might be due to the addition of Sr affecting the grain boundary conduction by acting as a grain boundary scavenger. As a result, the addition of strontium increases the total conductivity of pure GDC. Therefore, a material with low grain boundary resistance, i.e., high grain boundary conductivity, is ideal for practical applications. It has been reported by many investigators that the main contribution of the conductivity of ceria-based electrolytes in air was oxide ion conductivity, and hence the measured conductivity in air of the given co-doped ceria electrolyte was also solely considered as the oxide ion conductivity [5].

To confirm the scavenging effect of strontium for grain boundary, the influence of the grain boundary conductivity in the total conductivity is evaluated through the blocking factor (α_R) [20, 21] defined from the impedance diagram parameters by:

$$\alpha_R = R_{gb}/\left(R_g + R_{gb}\right) \quad (1)$$

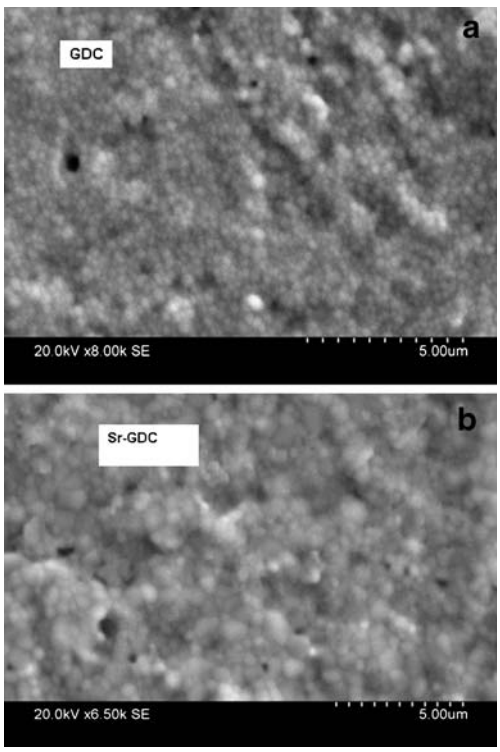

Fig. 4 **a** Scanning electron micrograph of as-sintered surface of GDC sample. **b** Scanning electron micrograph of as-sintered surface of Sr-GDC sample

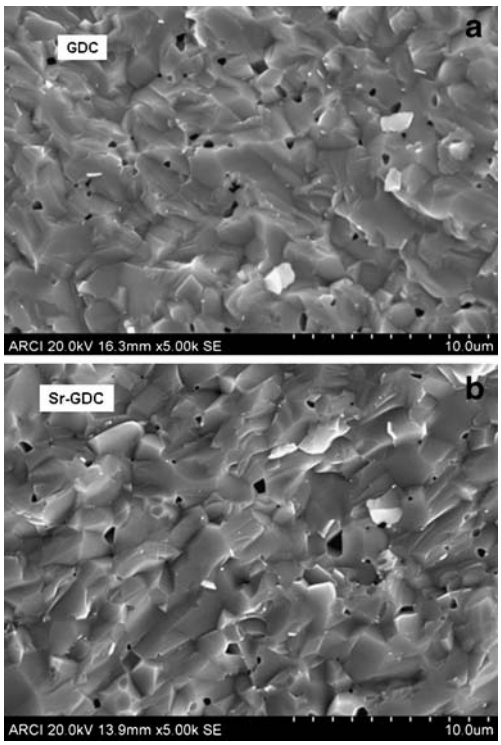

Fig. 5 **a** Scanning electron micrograph of fractured surface of GDC sample. **b** Scanning electron micrograph of fractured surface of Sr-GDC sample

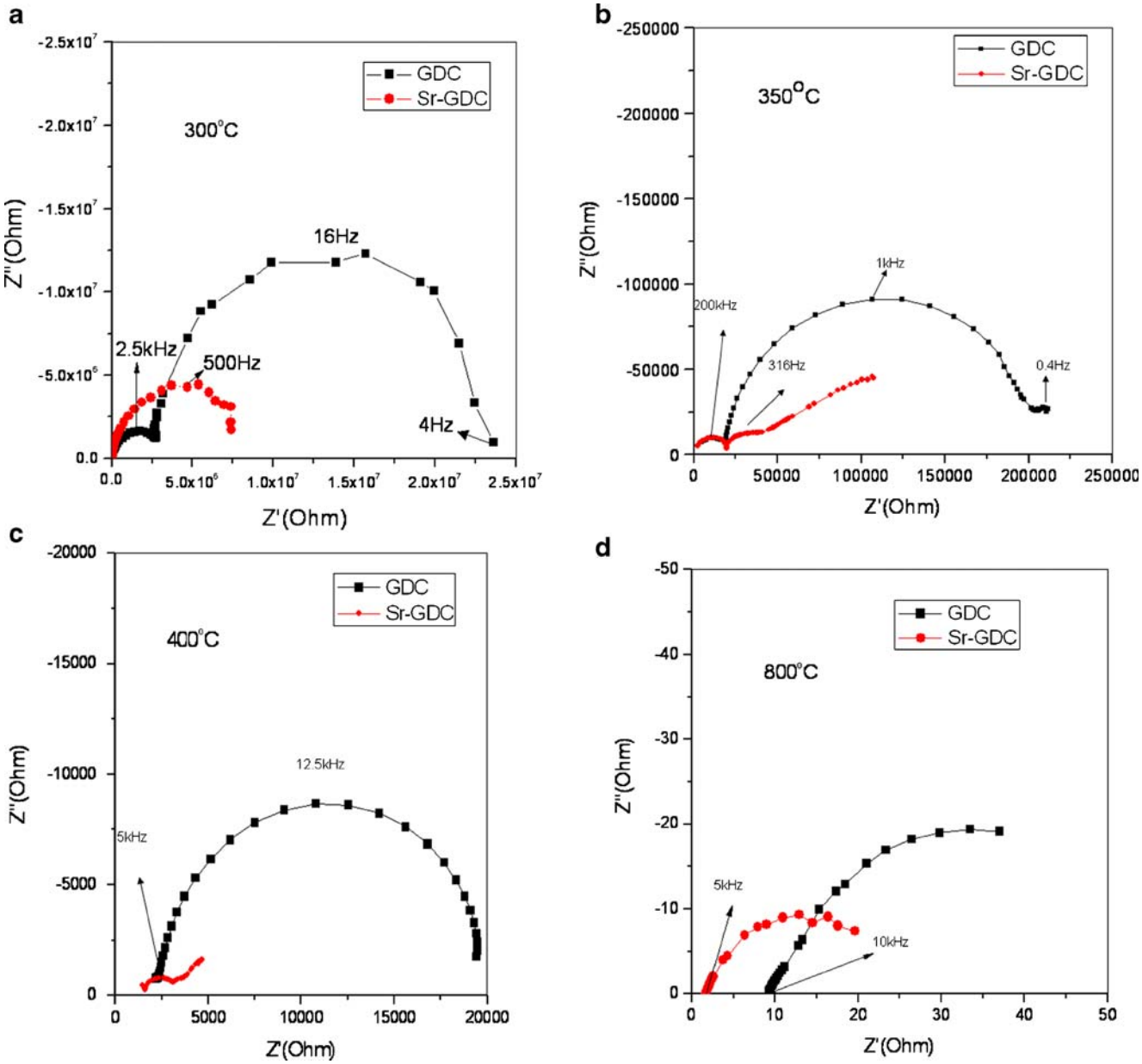

Fig. 6 **a** Cole–Cole plots recorded for GDC and Sr-GDC samples at 300°C in air. **b** Cole–Cole plots recorded for GDC and Sr-GDC samples at 350°C in air. **c** Cole–Cole plots recorded for GDC and Sr-GDC samples at 400°C in air. **d** Cole–Cole plots recorded for GDC and Sr-GDC samples at 800°C in air

where R_g and R_{gb} are grain and grain boundary resistances, respectively. This factor gives the fraction of the electric carriers being blocked at the impermeable internal surfaces, under the measuring conditions, with respect to the total number of electric carriers in the sample. The lowest blocking factor was observed in Sr-GDC sample (0.49 at 350°C against 0.9 for GDC). The assumption is that the observed blocking effect in stabilized ceria results directly from the formation of blocked zones, where electric carriers are trapped and do not contribute to the transport of electric current. This result clearly demonstrates that strontium is an effective scavenger of grain boundary and suggests that the addition of strontium promotes the grain boundary conduction and hence the total conduction in GDC [22].

The size of bulk and GB semicircles decreases with an increase of temperature. From the analysis of impedance patterns, the grain and the grain boundary conductivities were determined. The ionic conductivity of GDC was significantly enhanced by strontium addition. This might be due to increase in oxygen ion mobility with increasing temperature. The total conductivity of Sr-GDC (2.3×10^{-4}S/cm) at 400°C is higher than the reported result [15] and the conductivity values reported in this work are higher than those reported by Zhou et al. [23] and Dikmen et al. [24]. The conductivity of GDC

at 800°C is 0.028 S/cm and it has increased to 0.072 S/cm by the addition of strontium, which is three times higher than that of pure GDC. The respective values of the conductivities at different temperatures are given in the Table 1. Previous studies also reported an increase in ionic conductivity as a result of substitutions. A small increase of ionic conductivity was reported by the introduction of yttria into ceria–samaria solid solution [25]. A partial substitution of gadolinia by samaria in $Ce_{0.85}Gd_{0.15-x}Sm_xO_2$ up to $x=0.05$ also improves the total electrical conductivity compared to only ceria-doped gadolinia ($Ce_{0.85}Gd_{0.15}O_2$). A small ionic size mismatch between the host and a dopant was reported as a factor to enhance the ionic conductivity [26]. The critical ionic radius of the dopant was also cited as a factor for the change in ionic conductivity [1]. In addition to the single species doping in ceria, co-doping also increased the ionic conductivity [27]. An increase in oxygen vacancy radius with strontium doping in SDC was reported [19]. It is explained that oxygen ion migrates easily following oxygen vacancy radius enhancement. In the present study, the increase in ionic conductivity by strontium addition in GDC might be due to enhancement in the number of oxygen vacancies, with strontium acting as grain boundary scavenger, in addition to oxygen vacancy radius and decrease in average binding energy [28].

Figure 7 shows the equivalent circuit for Sr-GDC electrolyte. It is composed of two parallel RC circuits, where the resistance R_g denotes as the grain resistance and R_{gb} as grain boundary resistance and a series resistance R_s. The corresponding capacitances of grain and grain boundary are C_g and C_{gb}. Grain and grain boundary resistances are used to calculate the ionic conductivity of the samples. The total electrical conductivities of GDC and Sr-GDC can be described in terms of an Arrhenius-type relationship, which is a plot of $\log(\sigma T)$ versus 1,000/T as shown in Fig. 8. The plot yields a straight line with slope $-E_a/k$, provided that the activation energy E_a is found to be independent of temperature. Sr-GDC showed higher conductivity than GDC at all temperatures with more difference in the lower temperature ranges. The activation energies of the total conductivity for GDC and Sr-GDC were estimated to be 0.73 and 0.59 eV, respectively. These activation energies are lower than the earlier reports available in the literature [23, 24, 29]. According to Steele, the activation energy for conductivity of pure GDC is around 0.64 eV [30]. The addition of Sr^{2+} content to SDC enhances the amount of oxygen vacancies and decreases the association enthalpy and activation energy of SDC [19].

A higher oxide ionic conductivity is expected from a system containing a high concentration of oxygen vacancies, but with minimum average binding energy between dopant cation and anion vacancy. Substitution of lower-valent Sr^{2+} ions results in the creation of oxygen vacancies. Hideko et al. reported the decrease in the binding energy in GDC with the

Table 1 Ionic conductivity data of GDC and Sr-GDC samples in the temperature range 500–800°C

Operation temperature (°C)	GDC (ionic conductivity, S/cm)	Sr-GDC (ionic conductivity, S/cm)
500	0.00071	0.008
600	0.0051	0.013
700	0.0102	0.023
800	0.028	0.072

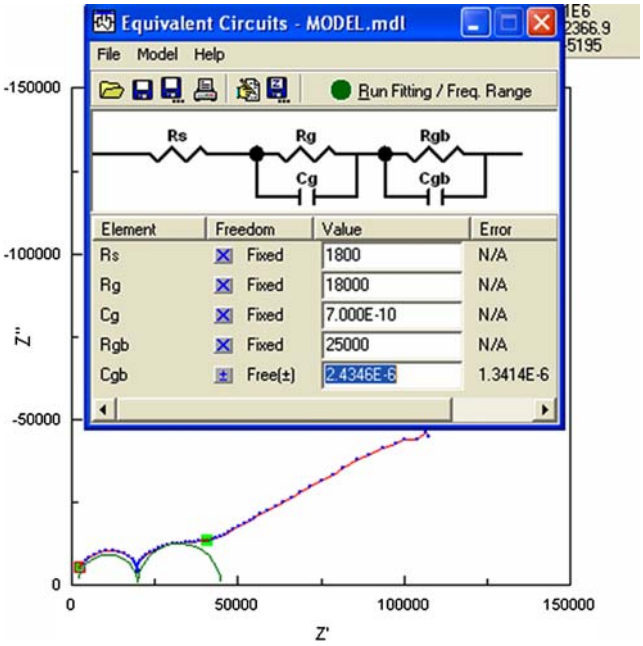

Fig. 7 Equivalent circuit with fitted Cole–Cole plot using Z-view software of Sr-GDC sample

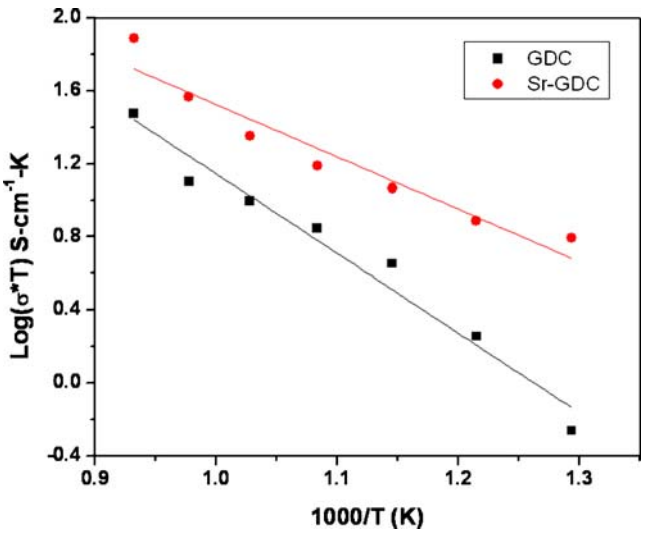

Fig. 8 Arrhenius plots of GDC and Sr-GDC samples

increase of oxygen vacancies [31]. This indicates that the addition of lower-valent Sr^{2+} ions reduced the average lattice binding energy of Sr-GDC. Thus, strontium doping to GDC lattice not only increases the oxygen vacancies but also results in the decrease of the lattice binding energy which in turn increases the oxygen ion mobility, leading to the observed threefold enhancement of electrical conductivity in comparison to un-doped GDC samples. Based on our experimental results, it could be concluded that co-doping was very effective to design new oxide-ion-conducting materials with better chemical stability against reduction compared to pure ceria and improved ionic conducting properties.

Conclusions

Strontium doping to GDC lattice acts as a sintering aid as is evident from the dilatometric and density determinations though there is a marginal increase in grain growth. The addition of strontium of only 1 wt% was found to enhance the densification and grain growth of GDC samples. The threefold increase in ionic conductivity of Sr-GDC can be attributed to improved density and increased grain size, leading to decrease in grain boundary area and resulting in the enhancement of total conductivity (σ_{700C}=0.072 S/cm). Further, strontium (Sr^{2+}) doping to GDC lattice not only increases the oxygen vacancies but also decreases the lattice binding energy, leading to increase in oxygen ion mobility. This is also confirmed by the relatively low activation energy exhibited by Sr-GDC (E_a=0.59eV). In conclusion, an effective way to improve the oxide ion conductivity of ceria-based oxides by co-doping was achieved.

References

1. Inaba H, Tagawa H (1996) Solid State Ionics 83:1
2. Kharton V, Figueiredo F, Navarro L, Naumovich E, Kovalevsky A, Yaremchenko A, Viskup A, Carneiro A, Margues M, Frade J (2001) J Mater Sci 36:1105
3. Sameshima S, Hirata Y, Ehira Y (2006) J Alloy Compd 408–412:628
4. Hong J, Mehta KJ (1998) J Electrochem Soc 145:638
5. Sujatha Devi P, Banerjee S (2008) Ionics 14:73
6. Lubke S, Wiemhofer HD (1999) Solid State Ionics 117:229
7. Kim N, Kim BH, Lee D (2000) J Power Sources 90:139
8. Lewis GS, Atkinson A, Steele BCH, Drennan J (2002) Solid State Ionics 152–153:567
9. Wang FY, Chen S, Wang Q, Yu S, Cheng S (2004) Catal Today 97:189
10. Wang FY, Chen S, Cheng S (2004) Electrochem Commun 6:743
11. Mori T, Drennan J, Lee JH, Li JG, Ikegami T (2002) Solid State Ionics 154/155:461
12. Yoshida H, Deguchi H, Miura K, Horiuchi M, Inagaki T (2001) Solid State Ionics 140:191
13. Zhang T, Hing P, Huang H, Kilner J (2001) J Eur Ceram Soc 21:2211
14. Zhang TS, Ma J, Leng YJ, Chang SH, Hing P, Kilner JA (2004) Solid State Ionics 168:187
15. Zhang T, Zeng Z, Huang H, Hing P, Kilner J (2002) Mater Lett 57:124
16. Tianshu Z, Hing P, Huang H, Kilner J (2001) Mat Sci Eng B 83:235
17. Fagg DP, Kharton VV, Frade JR (2002) J Electroceram 9:199
18. Kleinlogel C, Gauckler LJ (2000) Solid State Ionics 135:567
19. Tsung-Her Yeh and Chen-Chia Chou (2007) Phys Scripta T129:303
20. Gerhardt R, Nowick AS (1986) J Am Ceram Soc 69(9):641–646
21. Verkerk MJ, Middlehuis BJ, Burggraaf AJ (1982) Solid State Ionics 6:159
22. Chen XJ, Khor KA, Chan SH, Yu LG (2003) Mat Sci Eng A 341:4348
23. Zhou XD, Huebner W, Kosacki I, Anderson HU (2002) J Am Ceram Soc 85:1757
24. Dikmen S, Shuk P, Greenblatt M, Gocmez H (2002) Solid State Sci 4:585
25. Hung W, Shuk P, Greenblatt M (1998) Solid State Ionics 113–115:305
26. Catlow CRA (1984) Solid State Ionics 12:67
27. Bucko MM (2004) J Eur Ceram Soc 24:1305
28. Yoshida H, Inagaki T, Miura K, Inaba M, Ogumi Z (2003) Solid State Ionics 160:109
29. Arai H, Kunisaki T, Shimizu Y, Seiyama T (1986) Solid State Ionics 20:241
30. Steele BCH (2000) Solid State Ionics 129:95
31. Hideko H, Mariko K, Chang JQ, Hideaki I, Shaorong W, Masayuki D, Hiroaki T (2000) Solid State Ionics 132:227